UNIVERSITY OF BRADFORD
MAKING KNOWLEDGE WORK

Learner Support Services

The University of Bradford Institutional Repository

Author(s): Muscolino, G. and Palmeri, A.

Title: Response of beams resting on viscoelastically damped foundation to moving oscillators

"Response of beams resting on viscoelastically damped foundation to moving oscillators"

by

Giuseppe MUSCOLINO & Alessandro PALMERI

Response of Beams Resting on Viscoelastically Damped Foundation to Moving Oscillators

by Giuseppe Muscolino and Alessandro Palmeri

Department of Civil Engineering

University of Messina, Italy

Corresponding Author: Alessandro Palmeri

Department of Civil Engineering

University of Messina

Vill. S. Agata, 98166, Messina, Italy.

Tel: +39 090 397 7170, Fax: +39 090 397 7480

E-mail: <alexpalm@ingegneria.unime.it>

Abstract

The response of beams resting on viscoelastically damped foundation under moving SDoF oscillators is scrutinized through a novel state-space formulation, in which a number of internal variables is introduced with the aim of representing the frequency-dependent behaviour of the viscoelastic foundation. A suitable single-step scheme is provided for the numerical integration of the equations of motion, and the Dimensional Analysis is applied in order to define the dimensionless combinations of the design parameters that rule the responses of beam and moving oscillator. The effects of boundary conditions, span length and number of modes of the beam, along with those of the mechanical properties of oscillator and foundation, are investigated in a new dimensionless form, and some interesting trends are highlighted. The inaccuracy associated with the use of effective values of stiffness and damping for the viscoelastic foundation, as usual in the present state-of-practice, is also quantified.

1   Introduction

By virtue of the relevance in the analysis and design of railway tracks, the dynamic response of beams resting on elastic foundation and subjected to moving loads has been extensively investigated, and a number of experimental and numerical studies have been published in recent years (e.g. [1], [2] and the references provided therein).

The crudest approximation known to the literature is the so-called 'moving force' problem, in which the vehicle-track interaction in completely neglected, and the action of the vehicle is described as a concentrated force moving along the beam (e.g. [3], [4] and [5]). Also the case of beams on elastic foundation under moving loads has attracted engineers and researchers. Among the contributions published in the last decade, Thambiratnam and Zhuge [6] have used the Newmark integration scheme in order to scrutinize the effects of load speed, foundation stiffness and beam length on the dynamic amplification of the beam response. Felszeghy [7, 8] has analyzed the response to moving step loads by the Fourier transform method. Chen and Huang [9] have investigated the resonant velocity of infinite and finite railways subjected to harmonic loads.

More refined models are required when the phenomena of train-track interaction are dealt with. In particular, the solution of the so-called 'moving oscillator' problem, in which the vehicle is modelled as a SDoF oscillator of given mass, stiffness and damping, allows a qualitative evaluation of the interaction effects, which can be directly related to many engineering issues, e.g. damage in the track components and/or on the wheels. A reliable quantification of the train-track interaction necessitates, however, still more sophisticated approaches, in which each train vehicle is modelled as a MDoF system moving along the rail. In this way, for instance, the vibrations in a train crossing a railway bridge can be dependably predicted (e.g. [10] and [11]).

Despite the accuracy in modelling the train vehicles, however, the railway tracks are often handled with a very crude approximation, as elastic beams resting on a bed of elastic springs with a purely viscous damping. Actual tracks, on the contrary, exhibit a dynamic behaviour which may be much more complicated, with frequency-dependent stiffness and damping. As an example, this is the case of the track in the Milan subway, where a single

elastomeric pad is placed under the base-plate with the aim of mitigating the vibrations experienced by vehicles and track components [12]. In these situations the assumption of a mere viscous damping is inadequate, and more accurate rheological models should be considered in representing the viscoelastic behaviour of the foundation.

In the frequency domain the application of viscoelastic models is quite straightforward, and the mechanical impedance of a given track configuration can be easily evaluated once the properties of the elastomeric components are assigned. The vehicle-track interaction, however, lends itself to be effectively studied in the time domain. To do this, the equations governing the dynamic equilibrium of running vehicles and supporting track have to be coupled with the equations ruling the state variables of the viscoelastic components.

In this paper, the dynamic response of elastic beams resting on viscoelastically damped foundation to moving SDoF oscillators is coped with. The oscillator-beam-foundation interaction is investigated via a novel state-space formulation, in which the state variables are: the relative displacement and the relative velocity of the moving oscillator; the modal displacements and the modal velocities of the beam-foundation sub-system; the additional internal variables associated with the frequency-dependent response of the viscoelastic foundation.

Once the governing state-space equation is established, an effective single-step scheme is provided for the numerical integration. The Dimensional Analysis is successively applied in order to highlight the dimensionless combinations of the design parameters that control the response of the system under consideration. In the numerical examples, finally, the effects of boundary conditions, span length and number of modes of the supporting beam, along with those of the mechanical properties of moving oscillator and viscoelastic foundation are scrutinized, and some interesting trends are discussed.

2   Equations of motion

Let us considerer the dynamic system shown in Figure 1, made of a SDoF oscillator moving along an elastic beam resting on viscoelastic foundation.

The oscillator is made of a lumped mass, m_v, connected at one point only to the beam through a linear suspension. The latter is idealized as a Kelvin-Voigt element, made of an elastic spring, k_v, in parallel with a viscous dashpot, c_v. The position of the oscillator along the beam at a generic time instant, t, is described by the time law $x = x_v(t)$.

The beam is homogeneous, and extends from $x = 0$ to $x = L_b$. For the sake of simplicity, the Euler-Bernoulli model is assumed for the kinematics of the beam, although the extension to the Timoshenko model is quite easy. In addition to the span length, L_b, the mechanical parameters of the beam involved in the dynamic analysis are: the area, A_b, and the second moment, J_b, of the cross section; the mass density, ρ_b, and the Young modulus, E_b, of the material; the damping ratio, ζ_b, which is thought to be constant in all the modes of vibration of the beam.

The foundation is homogeneous too, and is represented in Figure 1 as a bed of springs, even if the response of these springs is assumed to be viscoelastic rather than purely elastic. The behaviour of the foundation, then, is fully defined by the dynamic stiffness, $K_f(\omega)$, which is a complex-valued function of the circular frequency, ω (e.g. [13] and [14]).

In a first stage, the moving oscillator and the elastic beam on viscoelastic foundation are handled as two non-interacting dynamic sub-systems, whose equations of motion are independently derived (Sections 2.1 and 2.2). In a second stage, the equilibrium and the compatibility conditions at the position of the moving oscillator are used in coupling the equations of motion (Sections 2.3 and 2.4), in so re-establishing the dynamic interaction among the two sub-systems.

2.1 Vibration of the beam

The motion of the beam in Figure 2a is governed by the partial differential equation:

$$\rho_b A_b\, \ddot{u}(x,t) + E_b J_b\, u''''(x,t) + D_b(x,t) = f(x,t) - K_f(\omega)\, u(x,t) \tag{1}$$

where the over-dot and the prime stand for the partial derivatives with respect to the time, t, and to the abscissa, x, respectively; $f(x,t)$ and $u(x,t)$ describe the time-dependent fields of transverse loads and transverse displacements, respectively; and $D_b(x,t)$ is the term associated

with the viscous damping in the beam. It is worth noting that Eq. (1) has been conveniently written in the so-called 'mixed' time-frequency domain, in which the dependence on the vibration frequency of the beam-foundation sub-system (also referred in this study as the 'continuum') is easily showed. Even if formally not rigorous, this way of writing the equations of motion allows to directly introduce the dynamic stiffness, which is the most popular experimental description of the viscoelastic components.

Once the motion of the beam is projected into the modal space, the field of the transverse displacements can be expressed as linear combination of the modal displacements:

$$u(x,t) = \sum_i \phi_i(x)\, q_i(t) \tag{2}$$

where $\phi_i(x)$ is the i-th modal shape of the continuum, and $q_i(t)$ is the associated modal displacement, which is ruled by the ordinary differential equation:

$$\ddot{q}_i(t) + 2\zeta_{\mathrm{b}}\,\omega_i\,\dot{q}_i(t) + \omega_i^2\,q_i(t) = \int_0^{L_{\mathrm{b}}} f(x,t)\,\phi_i(x)\,\mathrm{d}x - F_i(t) \tag{3}$$

$F_i(t)$ being the i-th modal force arising from the reaction of the viscoelastic foundation, $K_{\mathrm{f}}(\omega)\,u(x,t)$, from which the purely elastic portion, $K_{\mathrm{f}}(0)\,u(x,t)$, is subtracted; that is:

$$F_i(t) = \frac{K_{\mathrm{f}}(\omega) - K_{\mathrm{f}}(0)}{\rho_{\mathrm{b}} A_{\mathrm{b}}}\, q_i(t) \tag{4}$$

where the equilibrium modulus, $K_{\mathrm{f}}(0)$, is the stiffness of the foundation under static loads.

Once the boundary conditions are assigned, the i-th modal shape, $\phi_i(x)$, and the i-th modal circular frequency, ω_i, appearing in Eqs. (2) and (3) can be evaluated as solution of the eigenproblem:

$$\frac{E_{\mathrm{b}} J_{\mathrm{b}}}{\rho_{\mathrm{b}} A_{\mathrm{b}}}\phi_i''''(x) = \alpha_i\,\phi_i(x) \quad ; \quad \omega_i = \sqrt{\alpha_i + \frac{K_{\mathrm{f}}(0)}{\rho_{\mathrm{b}} A_{\mathrm{b}}}} \tag{5}$$

with the usual ortho-normal condition:

$$\rho_{\mathrm{b}} A_{\mathrm{b}} \int_0^{L_{\mathrm{b}}} \phi_i(x)\,\phi_k(x)\,\mathrm{d}x = \delta_{ik} \tag{6}$$

δ_{ik} being the Kronecker delta. It is worth noting that, since beam and foundation are homogeneous, the modal shape $\phi_i(x)$ and the eigenvalue α_i in the first of Eqs. (5) do not depend on the equilibrium modulus of the foundation; on the other hand, according to the second of Eqs. (5), the modal circular frequency ω_i increases with $K_f(0)$.

Eqs. (3) and (5) have been derived by extending to the case of continuous structures with distributed viscoelastic damping the method recently proposed by Palmeri *et al.* [15] for the modal analysis of steel frames provided with viscoelastic dampers. The method allows to carry out the dynamic analysis of structures with viscoelastic damping in a 'consistent' modal space, in which the actual rheological behaviour of the viscoelastic components is properly taken into account. Accordingly, the modal oscillators of a viscoelastically damped structure are SDoF dynamic systems featuring a damping which is viscoelastic rather than viscous. In Eq. (3), in particular, the modal force $F_i(t)$, given by Eq. (4), accounts for the effects of the frequency-dependent behaviour of the viscoelastic foundation on the i-th mode of vibration. When the viscoelastic components are distributed proportionally to mass and/or elastic stiffness of the structure, like in the beam-foundation sub-system considered in this study, the viscoelastic damping is 'classic'. The modal oscillators, then, vibrate independently, and the modal equations are uncoupled. The mathematical conditions to perfectly uncouple the modal equations can be found in Reference [16], in which the well-know Caughey–O'Kelly condition [17] is generalized to the case of viscoelastic damping.

2.2   *Vibration of the oscillator*

The vertical vibration of the SDoF oscillator of Figure 2b, moving along the beam, is ruled by:

$$m_v\,\ddot{v}_a(t) + c_v\dot{v}(t) + k_v v(t) = m_v\,g \tag{7}$$

where $\ddot{v}_a(t)$ is the absolute vertical acceleration of the mass of the oscillator, m_v; $v(t)$ and $\dot{v}(t)$ are the relative vertical displacement and velocity between oscillator and beam, respectively; and g is the intensity of the surrounding gravitational field.

When the oscillator is in contact with the beam $(0 \leq x_{\mathrm{v}}(t) \leq L_{\mathrm{b}})$, the absolute acceleration $\ddot{v}_{\mathrm{a}}(t)$ is the sum of the relative acceleration, $\ddot{v}(t)$, and of the acceleration of the beam at the contact point, given by $\mathrm{d}^2\, u(x_{\mathrm{v}}(t),t)\big/\mathrm{d}t^2$; otherwise absolute and relative accelerations coincide, i.e. $\ddot{v}_{\mathrm{a}}(t) \equiv \ddot{v}(t)$. Eq. (7), then, can be rewritten as:

$$\ddot{v}(t) + 2\,\zeta_{\mathrm{v}}\,\omega_{\mathrm{v}}\,\dot{v}(t) + \omega_{\mathrm{v}}^2 v(t) = g - \Upsilon_{\mathrm{v}}(t)\,\frac{\mathrm{d}^2}{\mathrm{d}t^2}\,u(x_{\mathrm{v}}(t),t) \tag{8}$$

where $\omega_{\mathrm{v}} = \sqrt{k_{\mathrm{v}}/m_{\mathrm{v}}}$ and $\zeta_{\mathrm{v}} = c_{\mathrm{v}}\big/(2\,\omega_{\mathrm{v}}\,m_{\mathrm{v}})$ are the circular frequency and the viscous damping ratio of the moving oscillator; and $\Upsilon_{\mathrm{v}}(t)$ is a window function, which gives 1 when oscillator and beam are in contact, 0 otherwise:

$$\Upsilon_{\mathrm{v}}(t) = U(x_{\mathrm{v}}(t))\,U(L_{\mathrm{b}} - x_{\mathrm{v}}(t))$$

$U(x)$ being the unit step function; that is: $U(x) = 1$ when $x \geq 0$, $U(x) = 0$ otherwise.

2.3   Compatibility

Eq. (8) satisfies the compatibility between the vibrations of supporting beam and moving oscillator, which is forced by the total acceleration of the continuum at the contact point. Since the latter moves along the beam according to the time law $x = x_{\mathrm{v}}(t)$, the total derivative in the r.h.s. of Eq. (8) brings:

$$\begin{aligned}
&\ddot{v}(t) + 2\,\zeta_{\mathrm{v}}\,\omega_{\mathrm{v}}\,\dot{v}(t) + \omega_{\mathrm{v}}^2 v(t) = g \\
&- \Upsilon_{\mathrm{v}}(t)\left[\ddot{u}(x_{\mathrm{v}}(t),t) + 2\,\dot{u}'(x_{\mathrm{v}}(t),t)\,\dot{x}_{\mathrm{v}}(t) + u''(x_{\mathrm{v}}(t),t)\,\dot{x}_{\mathrm{v}}^2(t) + u'(x_{\mathrm{v}}(t),t)\,\ddot{x}_{\mathrm{v}}(t)\right]
\end{aligned} \tag{9}$$

Then, substitution of Eq. (2) into Eq. (9) gives:

$$\ddot{v}(t) + 2\,\zeta_{\mathrm{v}}\,\omega_{\mathrm{v}}\,\dot{v}(t) + \omega_{\mathrm{v}}^2 v(t) = g - \sum_i \left\{ M_{\mathrm{v}i}(t)\,\ddot{q}_i(t) + C_{\mathrm{v}i}(t)\,\dot{q}_i(t) + K_{\mathrm{v}i}(t)\,q_i(t) \right\} \tag{10}$$

where the modal time-dependent coefficients $M_{\mathrm{v}i}(t) = \phi_i(x_{\mathrm{v}}(t))\,\Upsilon_{\mathrm{v}}(t)$, $C_{\mathrm{v}i}(t) = 2\,\phi_i'(x_{\mathrm{v}}(t))\,\dot{x}_{\mathrm{v}}(t)\,\Upsilon_{\mathrm{v}}(t)$ and $K_{\mathrm{v}i}(t) = [\phi_i''(x_{\mathrm{v}}(t))\,\dot{x}_{\mathrm{v}}^2(t) + \phi_i'(x_{\mathrm{v}}(t))\,\ddot{x}_{\mathrm{v}}(t)]\,\Upsilon_{\mathrm{v}}(t)$ are the mass, the viscous damping and the elastic stiffness, respectively, with which the i-th mode of the beam-foundation sub-system is coupled with the moving oscillator.

In order to satisfy the equilibrium between continuum and oscillator, the field of the transverse loads on the beam in Eq. (3), $f(x,t)$, is now expressed as the force in the suspension of the oscillator, localized at the contact point (see Fig. 2):

$$f(x,t) = \left[k_{\mathrm{v}}\, v(t) + c_{\mathrm{v}} \dot{v}(t) \right] \Upsilon_{\mathrm{v}}(t)\, \delta(x - x_{\mathrm{v}}(t)) \tag{11}$$

where $\delta(x)$ is the Dirac delta function. Then, substitution of Eq. (11) into Eq. (3) gives:

$$\ddot{q}_i(t) + 2\,\zeta_i\,\omega_i\,\dot{q}_i(t) + \omega_i^2\,q_i(t) = \Upsilon_{\mathrm{v}}(t)\left[k_{\mathrm{v}}\, v(t) + c_{\mathrm{v}} \dot{v}(t) \right] \phi_i(x_{\mathrm{v}}(t)) - F_i(t) \tag{12}$$

which shows that the moving oscillator forces the i-th mode of the continuum proportionally with $\phi_i(x_{\mathrm{v}}(t))$, which is the value of the i-th modal shape at the contact position.

3   Modelling the viscoelastic foundation

In the previous section the equations governing the coupled vibrations of moving oscillator and supporting beam on viscoelastic foundation are established, with the aim of simulating the dynamic interaction among train vehicles and railway track. A key aspect in this interaction proves to be the modelling of the track, where a central role is played by the elastomeric components, particularly in the case of non-ballasted tracks (e.g., Bruni and Collina [12] and references given therein). In this circumstance the use of a Kelvin-Voigt model, with equivalent values of elastic stiffness and viscous damping, cannot be considered fully adequate, since it is unable to reproduce the actual frequency-dependent behaviour of elastomeric components.

3.1   Rheological models

In the paper by Bruni and Collina [12], as an example, a non-ballasted track configuration, widely adopted in the Milan subway, has been experimentally and numerically investigated. In this configuration an additional viscoelastic damping is provided by a single elastomeric pad, which is placed under the base-plate (a sketch is displayed in Ref. [12]). It is found that simple

rheological models, given by the combinations of a few elementary components (elastic springs and viscous dashpots) allow to accurately reproduce the dynamic behaviour of the track.

Accordingly, in the following the so-called Standard Linear Solid (SLS) model, depicted in Figure 3a, is considered in representing the viscoelastic behaviour of the foundation. This model depends on three parameters only, being made of the elastic spring K_0, which gives the equilibrium modulus, and of a single Maxwell element in parallel, which is characterized by the stiffness K_1 and the relaxation time $\tau_1 = C_1/K_1$. The combination rules for series and parallel chains allow evaluating the dynamic stiffness of the SLS model as:

$$K(\omega) = K_0 + K_1 \frac{\tau_1\, \omega}{\tau_1\, \omega - \mathrm{j}} \tag{13}$$

$\mathrm{j} = \sqrt{-1}$ being the imaginary unit. Of course, more refined models, e.g. involving more than one Maxwell element (e.g. [18]), could be required in the real life. However, the extension of the proposed approach is quite straightforward; moreover, the simple SLS model is able to capture the main features of a wide variety of elastomeric materials of practical application.

Finally, one can also show that the SLS model is perfectly equivalent to the so-called elementary Zener model, depicted in Figure 3b and suggested in Ref. [12], once the four parameters k_1, k_2, k_3 and c_1 are properly set. Notice that, even if effective, the Zener model results to be over-parameterized, i.e. one stiffness among k_1, k_2 and k_3 is redundant. The SLS model, then, should be preferred in practical applications.

3.2   State equations

In the mixed time-frequency domain, the force-displacement relationship for any linear viscoelastic model can be posed in the form (e.g. Refs. [13] and [14]):

$$\bar{F}(t) = K(\omega)U(t)$$

where $U(t)$ is the time history of the displacement measured at the free end of the model, and $\bar{F}(t)$ is the time history of the total force experienced by the model, including the purely elastic portion, $K(0)U(t) = K_0 U(t)$. When the latter is removed, one obtains:

$$F(t) = \bar{F}(t) - K_0 U(t) = \left[K(\omega) - K_0\right] U(t) \tag{14}$$

which is in the same form as in Eq. (4).

When a linear viscoelastic model is obtained as chain of springs and dashpots, the force $F(t)$ can be expressed as a linear combination of a certain number of state variables, ruled by linear equations. In the case of the SLS model, in particular, the state equations are well-known to the literature (e.g. Palmeri *et al.* [18]), and can be posed in the form:

$$F(t) = K_1 \lambda_1(t) \quad ; \quad \dot{\lambda}_1(t) = \dot{U}(t) - \frac{\lambda_1(t)}{\tau_1} \tag{15}$$

where $\lambda_1(t)$ is an additional internal variable, measuring the strain in the spring K_1 of the single Maxwell element. It is worth noting that no approximations are introduced in this way, since Eqs. (15) give the exact reaction force experienced in the Maxwell element.

4   State-space formalism

In previous sections the equations governing the modal responses of the continuum (Eq. (12)), the vibration of the oscillator (Eq. (10)) and the response of the SLS viscoelastic model (Eqs. (15)) are established. Aim of this section is to couple these equations in a compact state-space form. Afterwards, an effective numerical scheme is provided which enables the dynamic responses of continuum and oscillator to be simultaneously evaluated in the time domain.

4.1   Coupled equations of motion

In a first stage Eqs. (12) and (10) can be posed in a matrix form, once the state arrays $\mathbf{z}_i(t) = \left[q_i(t) \quad \dot{q}_i(t)\right]^{\mathrm{T}}$ for the i-th mode of the supporting beam-foundation sub-system and $\mathbf{z}_{\mathrm{v}}(t) = \left[v(t) \quad \dot{v}(t)\right]^{\mathrm{T}}$ for the moving oscillator are defined. In doing so, Eq. (12) brings:

$$\dot{\mathbf{z}}_i(t) = \mathbf{D}_i \, \mathbf{z}_i(t) + \mathbf{D}_{iv}(t) \, \mathbf{z}_{\mathrm{v}}(t) - \mathbf{v} \, F_i(t) \tag{16}$$

where:

$$\mathbf{D}_i = \begin{bmatrix} 0 & 1 \\ -\omega_i^2 & -2\zeta_i\,\omega_i \end{bmatrix} \quad ; \quad \mathbf{D}_{iv}(t) = \phi_i(x_{\mathrm{v}}(t))\,\Upsilon_{\mathrm{v}}(t) \begin{bmatrix} 0 & 0 \\ k_{\mathrm{v}} & c_{\mathrm{v}} \end{bmatrix} \quad ; \quad \mathbf{v} = \begin{bmatrix} 0 \\ 1 \end{bmatrix}$$

Analogously, after some algebra, Eq. (10) brings:

$$\dot{\mathbf{z}}_v(t) = \mathbf{D}_v\,\mathbf{z}_v(t) + \mathbf{v}\,g + \sum_i \Big[\mathbf{D}_{vi}(t)\,\mathbf{z}_i(t) - \mathbf{v}\,M_{vi}(t)\,\mathbf{v}^{\mathrm{T}}\,\dot{\mathbf{z}}_i(t) \Big] \qquad (17)$$

where:

$$\mathbf{D}_v = \begin{bmatrix} 0 & 1 \\ -\omega_v^2 & -2\,\zeta_v\,\omega_v \end{bmatrix} \quad ; \quad \mathbf{D}_{vi}(t) = \begin{bmatrix} 0 & 0 \\ -K_{vi}(t) & -C_{vi}(t) \end{bmatrix}$$

In order to eliminate in the r.h.s. of Eq. (17) the time derivative of the modal state arrays $\mathbf{z}_i(t)$, Eq. (16) is substituted, so giving:

$$\dot{\mathbf{z}}_v(t) = \bar{\mathbf{D}}_v(t)\,\mathbf{z}_v(t) + \sum_i \bar{\mathbf{D}}_{vi}(t)\mathbf{z}_i(t) + \mathbf{v}\,g + \mathbf{v}\sum_i \Big[M_{vi}(t)\,F_i(t) \Big] \qquad (18)$$

where:

$$\bar{\mathbf{D}}_v(t) = \mathbf{D}_v - \mathbf{v}\,\mathbf{v}^{\mathrm{T}}\sum_i M_{vi}(t)\,\mathbf{D}_{iv}(t) \quad ; \quad \bar{\mathbf{D}}_{vi}(t) = \mathbf{D}_{vi}(t) - \mathbf{v}\,\mathbf{v}^{\mathrm{T}} M_{vi}(t)\,\mathbf{D}_i$$

In a second stage, the comparison between Eqs. (4), (14) and (15) shows that an additional internal variable, namely $\lambda_{i1}(t)$, has to be introduced for the i-th mode of vibration of the continuum. As a consequence, when the first m modes are retained in the dynamic analysis, m additional internal variables, i.e. $\lambda_{11}(t)$, $\lambda_{21}(t)$, $\cdots$ and $\lambda_{m1}(t)$, have to be considered. By using these new quantities, the i-th modal force associated with the reaction of the foundation, $F_i(t)$, can be expressed as:

$$F_i(t) = \frac{K_1}{\rho_b\,A_b}\,\lambda_{i1}(t) \qquad (19)$$

where $\lambda_{i1}(t)$ can be viewed as the strain in the spring K_1 of the SLS model (Fig. 3a) associated with the effects of the viscoelastic foundation on the i-th mode of vibration of the beam. By virtue of the second of Eqs. (15), moreover, this additional internal variable is ruled by:

$$\dot{\lambda}_{i1}(t) = \dot{q}_i(t) - \frac{\lambda_{i1}(t)}{\tau_1} \qquad (20)$$

Eqs. (16), (18), (19) and (20) have to be solved simultaneously. To this end, let us considerer the super-array listing the state variables of the coupled oscillator-beam-foundation system:

$$\mathbf{z}(t) = \left[\mathbf{z}_v^T(t) \mid \mathbf{z}_1^T(t) \quad \cdots \quad \mathbf{z}_m^T(t) \mid \lambda_{11}(t) \quad \cdots \quad \lambda_{m1}(t) \right]^T \tag{21}$$

which is ruled by the state-space equation:

$$\dot{\mathbf{z}}(t) = \mathbf{D}(t)\,\mathbf{z}(t) + \mathbf{f} \tag{22}$$

where the time-dependent dynamic matrix, $\mathbf{D}(t)$, and the constant forcing array, $\mathbf{f}$, take the expressions:

$$\mathbf{D}(t) = \left[\begin{array}{cccc|ccc}
\bar{\mathbf{D}}_v(t) & \bar{\mathbf{D}}_{v1}(t) & \cdots & \bar{\mathbf{D}}_{vm}(t) & \dfrac{M_{v1}(t)\,K_1}{\rho_b\,A_b}\mathbf{v} & \cdots & \dfrac{M_{vm}(t)\,K_1}{\rho_b\,A_b}\mathbf{v} \\
\hline
\mathbf{D}_{1v}(t) & \mathbf{D}_1 & & & -\dfrac{K_1}{\rho_b\,A_b}\mathbf{v} & & \\
\vdots & & \ddots & & & \ddots & \\
\mathbf{D}_{mv}(t) & & & \mathbf{D}_m & & & -\dfrac{K_1}{\rho_b\,A_b}\mathbf{v} \\
\hline
[0 \; 0] & \mathbf{v}^T & & & 1/\tau_1 & & \\
\vdots & & \ddots & & & \ddots & \\
[0 \; 0] & & & \mathbf{v}^T & & & 1/\tau_1
\end{array} \right] \quad ; \quad \mathbf{f} = \left[\begin{array}{c}
\mathbf{v}\,g \\
\hline
\begin{bmatrix} 0 & 0 \end{bmatrix}^T \\
\vdots \\
\begin{bmatrix} 0 & 0 \end{bmatrix}^T \\
\hline
0 \\
\vdots \\
0
\end{array} \right] \tag{23}$$

When the initial conditions of the system are assigned, $\mathbf{z}(0) = \mathbf{z}_0$, along with the time law for the moving oscillator, $x = x_v(t)$, the solution of Eq. (22) furnishes at once the dynamic responses of beam, foundation and oscillator. Since the classical incremental solutions do not apply when the dynamic matrix is time-dependent, an efficient numerical scheme is proposed in the next sub-section.

4.2   Numerical scheme

Eq. (22) constitutes a set of $3\,m + 2$ first-order non-homogeneous linear differential equations, with time-dependent coefficients. The solution can be expressed in integral form as [19]:

$$\mathbf{z}(t) = \mathbf{\Theta}(t,0)\,\mathbf{z}_0 + \left[\int_0^t \mathbf{\Theta}(t,\tau)\,\mathrm{d}\tau\right]\mathbf{f} \qquad (24)$$

where $\mathbf{z}_0$ is the array listing the initial conditions of the state variables, and $\mathbf{\Theta}(t,\tau)$ is the two-time transition matrix associated with the time-dependent dynamic matrix $\mathbf{D}(t)$, given by the first of Eqs. (23). Unfortunately, Eq. (24) is not useful in practical applications, as numerical evaluation of the transition matrix and implementation of the convolution integral are too cumbersome.

The solution of Eq. (22), then, can be sought by the single-step scheme herein presented. Let the time axis be subdivided into 'small' intervals of equal length, Δt. More precisely, Δt should be sufficiently small when compared with the time scales of oscillator, beam, foundation and time law of the transit, e.g.:

$$\Delta t = \min\left\{\frac{1}{8}\frac{2\pi}{\omega_\mathrm{v}}, \frac{1}{8}\frac{2\pi}{\omega_m}, \frac{1}{5}\tau_1, \frac{1}{50}\frac{L_\mathrm{b}}{\max\left\{\left|\dot{x}_\mathrm{v}(t)\right|\right\}}\right\}$$

where $2\pi/\omega_\mathrm{v}$ and $2\pi/\omega_m$ are the undamped periods of vibration of the moving oscillator and of the higher mode of the continuum, respectively; τ_1 is the relaxation time of viscoelastic foundation; and $\max\left\{\left|\dot{x}_\mathrm{v}(t)\right|\right\}$ stands for the maximum speed of the oscillator along the beam.

Since Δt is small, in the n-th time interval, $\left[t_n, t_{n+1}\right]$, being $t_n = n\,\Delta t$, the dynamic matrix can be assumed to be constant without appreciable loss of accuracy. In particular, let the n-th dynamic matrix to be $\mathbf{D}_n = \mathbf{D}(t_n + \Delta t/2)$, i.e. the coefficients of $\mathbf{D}_n$ take the values at the midpoint of the n-th time interval. In this interval, then, Eq. (22) can be re-written as:

$$\dot{\mathbf{z}}(t) = \mathbf{D}_n\,\mathbf{z}(t) + \left[\mathbf{D}(t) - \mathbf{D}_n\right]\mathbf{z}(t) + \mathbf{f} \quad , \quad t_n \le t \le t_{n+1} \qquad (25)$$

Eq. (25) can be conveniently viewed as a state-space equation with time-independent coefficients, forced by the constant array $\mathbf{f}$ and by an extra time-dependent term, $\left[\mathbf{D}(t) - \mathbf{D}_n\right]\mathbf{z}(t)$. The key point of the proposed numerical scheme is the assumption that this term varies linearly in the n-th time interval. Hence, the state arrays at the beginning, $\mathbf{z}_n = \mathbf{z}(t_n)$, and at the ending, $\mathbf{z}_{n+1} = \mathbf{z}(t_{n+1})$, can be related via the implicit equation:

$$z_{n+1} = \Theta_n z_n + L_n f + \Gamma_{n0}\left[D(t_n) - D_n\right]z_n + \Gamma_{n1}\left[D(t_{n+1}) - D_n\right]z_{n+1} \tag{26}$$

where the n-th transition matrix Θ_n can be easily computed as the exponential matrix of $D_n \Delta t$ [19]:

$$\Theta_n = \exp\left[D_n \Delta t\right]$$

and where the matrices L_n, Γ_{n0} and Γ_{n1} are given by [20]:

$$L_n = \left(\Theta_n - I_{3m+2}\right)D_n^{-1} \quad ; \quad \Gamma_{n0} = \left(\Theta_n - \tfrac{1}{\Delta t}L_n\right)D_n^{-1} \quad ; \quad \Gamma_{n1} = \left(\tfrac{1}{\Delta t}L_n - I_{3m+2}\right)D_n^{-1}$$

I_{3m+2} being the identity matrix of size $3m+2$. According to Muscolino [21], Eq. (26) can be solved with respect to z_{n+1}:

$$z_{n+1} = \hat{\Theta}_n z_n + \hat{L}_n f \tag{27}$$

where the 'modified' matrices $\hat{\Theta}_n$ and $\hat{L}_n$ are given by:

$$\hat{\Theta}_n = J_n\left\{\Theta_n + \Gamma_{n0}\left[D(t_n) - D_n\right]\right\} \quad ; \quad \hat{L}_n = J_n L_n$$

being $J_n = \left\{I_{3m+2} - \Gamma_{n1}\left[D(t_{n+1}) - D_n\right]\right\}^{-1}$.

5   Dimensionless combinations of the design parameters

The generic response of the dynamic system considered in this paper, e.g. the peak deflection of the supporting continuum or the maximum vertical acceleration experienced by the moving oscillator, can be viewed as an output variable, Q_0, which is a function of a large number of input variables, $Q_1 \dots Q_r$. The application of the Dimensional Analysis (see Appendix II), then, allows defining the dimensionless combinations of the design parameters which rule the response. As a result, the dependence on the input variables can be suitably simplified.

According to the procedure summarized in Appendix II, the complete set of the input variables in our problem is initially identified. The first input variable is the acceleration of gravity, $[g] = L\,T^{-2}$. For the beam we have four input variables: mass per unit length,

$\left[\rho_{\rm b} A_{\rm b}\right] = {\rm L}^{-1}\,{\rm M}$; flexural stiffness, $\left[E_{\rm b} J_{\rm b}\right] = {\rm L}^3\,{\rm M}\,{\rm T}^{-2}$; span length, $\left[L_{\rm b}\right] = {\rm L}$; and damping ratio, $\left[\zeta_{\rm b}\right] = 1$ (dimensionless). Three for the oscillator: mass, $\left[m_{\rm v}\right] = {\rm M}$; undamped circular frequency of vibration, $\left[\omega_{\rm v}\right] = {\rm rad}\,{\rm T}^{-1}$ (radians are dimensionless); and damping ratio, $\left[\zeta_{\rm v}\right] = 1$. Three for the foundation, described by the SLS model: equilibrium modulus, $\left[K_0\right] = {\rm L}^{-1}\,{\rm M}\,{\rm T}^{-2}$; stiffness of the Maxwell element, $\left[K_1\right] = {\rm L}^{-1}\,{\rm M}\,{\rm T}^{-2}$; and relaxation time, $\left[\tau_1\right] = {\rm T}$. Finally, in the simplest case where the speed $\dot{x}_{\rm v}$ of the oscillator is constant, there is one more input variable: the travelling time, $\left[T_{\rm tr} = L_{\rm b}/\dot{x}_{\rm v}\right] = {\rm T}$. Altogether, then, $r = 12$ input variables (design parameters) rule the response in our study, whose dimensions are in the form $[Q_i] = {\rm L}^{N_{il}}\,{\rm M}^{N_{im}}\,{\rm T}^{N_{it}}$ $(i = 1, \cdots, r)$, where ${\rm L}$, ${\rm M}$ and ${\rm T}$ are base units of length, mass and time, respectively. Among the several suitable choices, the $s = 3$ input variables $\rho_{\rm b} A_{\rm b}$, $E_{\rm b} J_{\rm b}$ and g are selected in constituting the complete subset of dimensionally independent variables. In practical railway applications, in fact, $\rho_{\rm b} A_{\rm b}$ and $E_{\rm b} J_{\rm b}$ are preventively selected, and $g = 9.81\,{\rm m/s}^2$ takes a fixed values.

Once the dimensionally independent variables are chosen, Eq. (A.34) is applied in order to define the independent dimensionless combinations: $\Pi_1 = L_{\rm b}\sqrt[3]{\rho_{\rm b} A_{\rm b}\,g/E_{\rm b} J_{\rm b}}$, which controls the span length of the supporting beam; $\Pi_2 = \zeta_{\rm b}$ (the damping ratio is dimensionless); $\Pi_3 = m_{\rm v}\sqrt[3]{g/\left(\rho_{\rm b}^2 A_{\rm b}^2\,E_{\rm b} J_{\rm b}\right)}$, which gives the dimensionless mass of the moving oscillator; $\Pi_4 = \omega_{\rm v}\sqrt[6]{E_{\rm b} J_{\rm b}/\left(\rho_{\rm b} A_{\rm b}\,g^4\right)}$, which measures the circular frequency of the oscillator in radians; $\Pi_5 = \zeta_{\rm v}$; $\Pi_6 = T_{\rm tr}\sqrt[6]{\rho_{\rm b} A_{\rm b}\,g^4/\left(E_{\rm b} J_{\rm b}\right)}$, which gives the travelling time of the moving oscillator; $\Pi_7 = K_0\sqrt[3]{E_{\rm b} J_{\rm b}/\left(\rho_{\rm b} A_{\rm b}\,g\right)^4}$ and $\Pi_8 = K_1\sqrt[3]{E_{\rm b} J_{\rm b}/\left(\rho_{\rm b} A_{\rm b}\,g\right)^4}$, whose values control the stiffness of the foundation; $\Pi_9 = \tau_1\sqrt[6]{\rho_{\rm b} A_{\rm b}\,g^4/\left(E_{\rm b} J_{\rm b}\right)}$, which gives the relaxation time of the foundation.

6   Numerical examples

The numerical scheme of Eq. (27), implemented in a Mathematica 4.0 [22] code, is applied in order to scrutinize the effects of the design parameters on the dynamic response of the oscillator-beam-foundation system. It is also quantified the inaccuracy associated with the use of an equivalent Kelvin-Voigt model in representing the viscoelastic foundation. To do this, the so-called Modal Strain Energy (MSE) method is applied (see Appendix I). Noticeably, the

MSE method, originally proposed by Johnson and Kienholz [23] for the analysis of structures with constrained viscoelastic layers, is the most popular one in the dynamic analysis of viscoelastically damped structures. Even though straightforward, however, this method proves to be inaccurate is some engineering situations (e.g., Refs. [15], [24] and [25]), and then should be carefully adopted.

6.1   Numerical values of the design parameters

In the numerical analyses the beam is assumed to be the UIC60 European high-speed rail, which has the following properties [9]: $\rho_b = 7850 \text{ kg/m}^3$, $E_b = 2.00 \times 10^7 \text{ N/cm}^2$, $A_b = 76.9 \text{ cm}^2$, $J_b = 3060 \text{ cm}^4$. Since all these quantities are used in defining the subset of dimensionally independent variables in our problem, the dimensionless results displayed in the following can be directly extended to different track configurations once the current values of mass per unit length, $\rho_b A_b$, and flexural stiffness, $E_b J_b$, are considered.

Both Simply-Supported (SS) and Clamped-Clamped (CC) boundary conditions are investigated. In our analyses the span length, L_b, varies from 5 to 40 m: for actual track configurations, in fact, convergence studies prove that beams of span length $L_b \geq 10$ m can accurately approximate the response of the ideal beam of infinite length [6]. Then, the first dimensionless combination, $\Pi_1 \propto L_b$, varies from 0.230 ('short' beam) to 1.84 ('long' beam). The damping ratio of the beam is assumed to be zero, i.e. $\Pi_2 = 0$.

The mass of the moving oscillator m_v is assumed to vary from 100 to 500 kg: as a consequence the third dimensionless combination, $\Pi_3 \propto m_v$, varies from 0.0761 ('light' oscillator) to 0.380 (heavy oscillator). The fundamental circular frequency of actual train vehicles, ω_v in our simple model, varies from 5 to 25 rad/s; accordingly, the fourth dimensionless combination, $\Pi_4 \propto \omega_v$, varies from 7.45 ('flexible' oscillator) to 37.3 rad ('stiff' oscillator). Also the damping ratio of the oscillator is assumed to be zero, i.e. $\Pi_5 = 0$. The travelling time, T_{tr}, is assumed to be one second, and then the sixth dimensionless combination, $\Pi_6 \propto T_{tr}$, takes the constant value 0.671.

According to Ref. [6], the equilibrium modulus of the rail foundation, K_0, varies from 5.20×10^6 to $3.54 \times 10^7 \text{ N/m}^2$. As a consequence, the seventh dimensionless combination,

$\Pi_7 \propto K_0$, varies from 1.91×10^5 ('soft' foundation) to 1.30×10^6 ('stiff' foundation). The viscoelastic behaviour of the foundation is governed by the last two dimensionless combinations, $\Pi_8 = \left(K_1/K_0 \right) \Pi_7$ and $\Pi_9 \propto \tau_1$. In order to define realistic values of these quantities, we refer to the experimental results displayed in Ref. [12], in which 'low-frequency' tests show that the equivalent stiffness (the 'storage modulus') of the elastomeric pad, $\text{Re}\left[K_{\text{f}}(\omega) \right]$, monotonically increases with the frequency of vibration, approximately from $2.0 \times 10^7 \text{ N/m}$ at $\omega = 31.4 \text{ rad/s}$, to $2.7 \times 10^7 \text{ N/m}$ at $\omega = 628 \text{ rad/s}$. These can be assumed as the limiting values of the storage modulus when the frequency goes to zero (equilibrium modulus) and when the frequency goes to infinity, respectively. When the elastomeric foundation is modelled with the SLS model (Eq. (13)) we have $K_{\text{f}}(0) = K_0$ and $K_{\text{f}}(\infty) = K_0 + K_1$, from which one computes $K_0 = 2.0 \times 10^7 \text{ N/m}$ and $K_1 = 0.7 \times 10^7 \text{ N/m}$. If the ratio $K_1/K_0 = 0.7/2.0 = 0.35$ is assumed to be constant, it follows that $\Pi_8 = 0.35 \, \Pi_7$.

More complicated is the assessment of the last dimensionless combination. The experimental results presented in Ref. [12], in fact, demonstrate that the elastomeric pad used in the Milan subway is almost 'hysteretic,' as the 'loss factor' of the foundation, $\eta_{\text{f}}(\omega) = \text{Im}\left[K_{\text{f}}(\omega) \right] / \text{Re}\left[K_{\text{f}}(\omega) \right]$, increases slowly with the vibration frequency, approximately from 0.15 at $\omega = 31.4 \text{ rad/s}$ to 0.21 at $\omega = 628 \text{ rad/s}$. Recent studies demonstrated that the use of more refined state-space viscoelastic models, e.g. the 'Generalized Maxwell model' [26] and the LPA (Laguerre Polynomial Approximation) technique [27], enable the time-domain dynamic analysis of linear hysteretic structures. Since the SLS model is too simple to accurately fit the experimental data, nevertheless in our analyses it is assumed that the relaxation time varies from 0.001 to 1 s, in so covering all the situations of practical interest; as a consequence, the dimensionless combination Π_9 varies from 6.71×10^{-4} to 0.671.

6.2   *Eigenproperties of the continuum: effects of boundary conditions and span length*

The eigenproperties (modal frequencies and modal shapes) of the beam-foundation sub-system are evaluated according to Eqs. (5) and (6). Once the boundary conditions of the beam at $x = 0$ and $x = L_{\text{b}}$ are specified, the first of Eqs. (5) gives modal shapes and

characteristic equation. In particular, when the beam is Simply Supported (SS) at the ends, the i-th modal shape takes the expression:

$$\phi_i(x) = A_i \sin\left(\gamma_i\, x/L_b\right) \quad , \quad i = 1, 2, \cdots \tag{28}$$

and the characteristic equation is $\sin(\gamma) = 0$, whose non-trivial solutions are $\gamma_i = i\pi$. When the beam is Clamped-Clamped (CC) at the ends, the i-th modal shape is:

$$\begin{aligned}
\phi_i(x) = A_i \Big\{ &\left[\sin\left(\gamma_i\right) - \sinh\left(\gamma_i\right)\right]\left[\cos\left(\gamma_i\, x/L_b\right) - \cosh\left(\gamma_i\, x/L_b\right)\right] \\
&- \left[\cos\left(\gamma_i\right) - \cosh\left(\gamma_i\right)\right]\left[\sin\left(\gamma_i\, x/L_b\right) - \sinh\left(\gamma_i\, x/L_b\right)\right] \Big\} \quad , \quad i = 1, 2, \cdots
\end{aligned} \tag{29}$$

and the characteristic equation is $\cos(\gamma)\cosh(\gamma) = 1$, whose non-trivial solutions should be numerically computed: $\gamma_1 = 4.73$, $\gamma_2 = 7.85$, $\cdots$ (notice that $\gamma_i \cong (2i+1)\pi/2$ for $i > 2$). In both Eqs. (28) and (29) A_i is merely a normalization constant, whose value can be computed via Eq. (6) when $i = k$. In Figure 4 (top rows) the first six modal shapes of the beam for both SS (solid line) and CC (dashed line) boundary conditions are depicted in a dimensionless form; for each mode the values of the coefficients γ_i are also displayed.

Once the dimensionless coefficients γ_i are evaluated, the i-th eigenvalue in the first of Eqs. (5) takes the expression:

$$\alpha_i = \frac{E_b J_b}{\rho_b A_b L_b^4} \gamma_i^4$$

Since its dimensions are $[\alpha_i] = \mathrm{T}^{-2}$, the associated dimensionless value proves to be:

$$\alpha_i \sqrt[3]{\frac{E_b J_b}{\rho_b A_b g^4}} = \left(\frac{E_b J_b}{\rho_b A_b g}\right)^{\frac{4}{3}} \frac{\gamma_i^4}{L_b^4} = \left(\frac{\gamma_i}{\Pi_1}\right)^4$$

where Π_1 accounts for the mechanical characteristics of the beam, and the coefficients γ_i depend only on its boundary conditions.

The second of Eqs. (5) allows now evaluating the modal circular frequencies of the continuum. The i-th dimensionless value is given, in compact form, by:

$$\omega_i \sqrt[6]{E_b J_b \Big/ \left(\rho_b A_b\, g^4\right)} = \sqrt{\left(\frac{\gamma_i}{\Pi_1}\right)^4 + \frac{K_0}{\rho_b A_b}\sqrt[3]{\frac{E_b J_b}{\rho_b A_b\, g^4}}} = \sqrt{\left(\frac{\gamma_i}{\Pi_1}\right)^4 + \Pi_7} \qquad (30)$$

It is worth noting that the parametric investigation presented in the previous sub-section demonstrates that for the first modes of vibration the prevailing term in the r.h.s. of Eq. (30) is the dimensionless combination Π_7, which increases with the foundation stiffness.

The effects of boundary conditions and span length of the beam, which is measured by the dimensionless combination Π_1, are then investigated. In Figure 4 (centre rows) the dimensionless values of the first six modal circular frequencies (Eq. (30)) are displayed for Π_1 varying from 0.230 to 1.84, while the foundation is assumed to be soft (i.e. $\Pi_7 = 1.91 \times 10^5$). Interestingly, this analysis reveals that when $\Pi_1 \geq 1.00$ (i.e. $L_b \geq 21.8\,\mathrm{m}$ in the case of the selected UIC60 rail) the first three modal frequencies approach asymptotic values which are independent of the boundary conditions. The convergence is slightly slower when higher modes are considered.

For the comparison purposes, Eqs. (A.31) and (A.32) are also applied in order to compute the equivalent values of circular frequencies, $\tilde{\omega}_i$, and damping ratios, $\tilde{\zeta}_i$, given by the MSE method. These quantities reveal the same tendency, i.e. when $\Pi_1 \geq 1.00$ the asymptotic values are approached. In the following, then, the numerical analyses are conducted with $\Pi_1 = 1.00$. Moreover, given that the boundary conditions do not affect appreciably the eigenproperties of the continuum, in the following the beam is assumed to be SS at the ends.

Figure 4 (centre rows) demonstrates also that the equivalent circular frequencies $\tilde{\omega}_i$ in the MSE method are everywhere greater than the corresponding circular frequencies ω_i, as the viscoelastic damping in the foundation induces an apparent increase in the stiffness of the system. Finally, Figure 4 (bottom rows) shows that the effective damping ratio $\tilde{\zeta}_i$ provided by the viscoelastic foundation is slightly higher in the case of SS beams; furthermore, $\tilde{\zeta}_i$ tends to increase with the span length and to decrease in the higher modes.

6.3 Eigenproperties of the continuum: effects of the foundation characteristics

The effects of the dimensionless combinations Π_7 (equilibrium modulus) and Π_9 (relaxation time), which fully characterize the viscoelastic foundation, are scrutinized in

this sub-section. For the limiting values of the equilibrium modulus, i.e. $\Pi_7 = 1.91 \times 10^5$ (soft foundation, solid line) and $\Pi_7 = 1.30 \times 10^6$ (stiff foundation, dashed line), Figure 5 shows in log-linear form how dimensionless modal frequencies (centre rows) and effective damping ratios (bottom rows) vary with the relaxation time.

The plots reveal that the equivalent modal circular frequencies in the MSE method, $\tilde{\omega}_i$, increase monotonically with the relaxation time, approaching the asymptotic value for $\Pi_9 > 0.01$ (i.e., $\tau_1 > 0.0139$ s in the case of the selected UIC60 rail). In addition, it is worth noting that when the foundation is stiff (dashed line) the values of the first six modal frequencies are very close, since the prevailing contribution to the stiffness of the beam-foundation sub-system is due to the bed of viscoelastic springs.

More interesting is the behaviour of the effective modal damping ratios, $\tilde{\zeta}_i$. When the foundation is stiff (dashed line) $\tilde{\zeta}_i$ decreases monotonically with the relaxation time, and is almost constant for the first six modes of vibration. On the contrary, when the foundation is soft (solid line) $\tilde{\zeta}_i$ takes a maximum where $\Pi_9 = 0.002$ (i.e., $\tau_1 = 0.00298$ s), and decreases significantly in the higher modes.

6.4   Number of modes of the continuum

The accuracy of the response is investigated as a function of the number m of the modes of the continuum which are retained in the analysis. Figure 6 (left) shows the convergence in terms of the peak displacement of the beam, while Figure 6 (right) in terms of the peak absolute acceleration of the moving oscillator. In both cases for $m \geq 12$ the responses predicted by the proposed method (solid lines) and by the MSE method (dashed line) do not vary appreciably. Since the computational time exponentially increases with m, one can conclude that the use of $m = 12$ allows a good degree of accuracy with a tolerable computational effort. In the following, then, all the numerical analyses are conducted with $m = 12$ modes of vibration of the continuum. Moreover, it is worth noting that although the MSE method allows saving some computational time, the peak responses of beam and oscillator (Fig. 6) could be excessively underestimated. For instance, in the particular case considered   in   this   sub-section   ($\Pi_3 = 0.380$,   i.e.   heavy   oscillator, $\Pi_4 = 14.9$ rad,

$\Pi_7 = 1.91 \times 10^5$, i.e. soft foundation, and $\Pi_9 = 0.00336$) the inaccuracy of the MSE method is greater than 15%.

6.5   Response analysis: effects of mass and stiffness of the moving oscillator

The effects on the response of the dimensionless combination Π_3 and Π_4, which control the mass and the circular frequency of the moving oscillator, respectively, are scrutinized. Figure 7 shows that the peak responses of beam and oscillator increase linearly with the mass m_v, which is proportional to Π_3, and confirms that the MSE method is anticonservative. Figure 8 reveals that, in the selected range of values, the peak response of the beam is almost independent of ω_v, which is proportional to Π_4, while the peak response of the oscillator tends to increase with ω_v.

6.6   Response analysis: effects of the foundation characteristics

Finally, the effects on the response of the dimensionless combination Π_7 and Π_9, which control the equilibrium modulus and the relaxation time of the foundation, respectively, are investigated. Figures 9 and 10 show that, for the selected range of values, the peak responses of beam and oscillator reduce as the equilibrium modulus and the relaxation time increase. More interestingly, as a consequence of the apparent increase in the modal frequencies of the continuum, also in this case the MSE method (dashed line) proves to underestimate everywhere the peak responses.

7   Concluding remarks

A novel state-space formulation for evaluating the dynamic response of elastic beams resting on viscoelastically damped foundation to moving SDoF oscillators has been presented in this paper. The formulation is essentially devoted to investigate in the time domain the interaction between train vehicles and railway track, where viscoelastic components, e.g. elastomeric pads, are often introduced with the aim of mitigating the vibrations in vehicles and track. The main advantage is that, as opposite to the current state-of-practice (see Appendix I), the introduction of a number of additional internal variables in the complete state array (Eq. (21))

allows the proposed technique to consistently take into account the frequency-dependent behaviour of the viscoelastic foundation.

As the position of the oscillator on the beam varies with time, the dynamic matrix of the governing state-space equation is time-dependent (Eqs. (22) and (23)). Since the classical incremental solutions do not apply in this circumstance, an efficient single-step scheme has been provided for the numerical integration, based on a dynamic 'modification' in each time step (Eq. (27)). The proposed approach enables the dynamic responses of supporting continuum and moving oscillator to be simultaneously computed, once the twelve design parameters have been selected.

Since this number is too large to carry out parametric investigations of general interest, the so-called Buckingham Π-Theorem (see Appendix II) is applied in order to define the dimensionless combinations of the design parameters that control the response of the system under consideration. In doing so, the results of the dynamic analyses, presented in a convenient dimensionless form, can be directly extended to different track configurations.

The proposed procedure is amply illustrated by numerical examples, in which the effects of some important parameters, such as boundary conditions, span length, number of modes of the supporting beam, as well as dynamic characteristics of moving oscillator and viscoelastic foundation, are investigated in dept, and some interesting tendencies in the responses of beam and oscillator are highlighted. Finally, it is pointed out that the inaccuracy associated with the use of effective values of stiffness and damping for the foundation, widely adopted in the conventional techniques, could be unacceptable for engineering purposes.

Appendix I. State-space formalism with the MSE method

The Modal Strain Energy (MSE) method [23] is a general tool that allows defining the equivalent Kelvin-Voigt modal oscillators of a structure provided with viscoelastic components. According to this method, the effects of the viscoelastic foundation on the continuum considered in this study can be accounted for with equivalent values of the modal circular frequencies, $\tilde{\omega}_i \geq \omega_i$, and of the modal damping ratios, $\tilde{\zeta}_i \geq \zeta_i$, herein

denoted with an over-tilde. In particular, the circular frequency of the i-th mode of vibration is the root of the implicit equation:

$$\tilde{\omega}_i = \sqrt{\alpha_i + \frac{\text{Re}\big[K_\text{f}(\tilde{\omega}_i)\big]}{\rho_\text{b}\, A_\text{b}}} \tag{A.31}$$

where α_i is the i-th eigenvalue of the first of Eqs. (5). Once the root $\tilde{\omega}_i$ is numerically found, the damping ratio in the i-th mode of vibration is given by:

$$\tilde{\zeta}_i = \zeta_\text{b} + \frac{\text{Im}\big[K_\text{f}(\tilde{\omega}_i)\big]}{2\,\tilde{\omega}_i^2\, \rho_\text{b}\, A_\text{b}} \tag{A.32}$$

while the associated modal response is ruled by the equation:

$$\ddot{q}_i(t) + 2\,\tilde{\zeta}_i\, \tilde{\omega}_i\, \dot{q}_i(t) + \tilde{\omega}_i^2\, q_i(t) = \int_0^{L_\text{b}} f(x,t)\,\phi_i(x)\,\mathrm{d}x$$

In comparison with Eq. (3), the only formal difference is that in this case the i-th modal viscoelastic force, $F_i(t)$, is missed out. As a consequence, the state-space governing equation of the oscillator-beam-foundation system can be written in a form like Eq. (22):

$$\dot{\tilde{\mathbf{z}}}(t) = \tilde{\mathbf{D}}(t)\,\tilde{\mathbf{z}}(t) + \tilde{\mathbf{f}}$$

where the reduced super-array $\tilde{\mathbf{z}}(t) = \Big[\mathbf{z}_\text{v}^\text{T}(t) \ \Big|\ \mathbf{z}_1^\text{T}(t) \ \cdots \ \mathbf{z}_m^\text{T}(t)\ \Big|\Big]^\text{T}$ is of size $2m+2$, i.e. the m additional internal variables associated with the viscoelastic foundation are cut out, and where:

$$\tilde{\mathbf{D}}(t) = \left[\begin{array}{c|ccc} \bar{\mathbf{D}}_\text{v}(t) & \tilde{\bar{\mathbf{D}}}_{\text{v}1}(t) & \cdots & \tilde{\bar{\mathbf{D}}}_{\text{v}m}(t) \\ \hline \mathbf{D}_{1\text{v}}(t) & \tilde{\mathbf{D}}_1 & & \\ \vdots & & \ddots & \\ \mathbf{D}_{m\text{v}}(t) & & & \tilde{\mathbf{D}}_m \end{array}\right] \quad ; \quad \tilde{\mathbf{f}} = \left[\begin{array}{c} \mathbf{v}\,g \\ \hline \big[0 \ \ 0\big]^\text{T} \\ \vdots \\ \big[0 \ \ 0\big]^\text{T} \end{array}\right] \tag{A.33}$$

in which:

$$\tilde{\mathbf{D}}_i = \begin{bmatrix} 0 & 1 \\ -\tilde{\omega}_i^2 & -2\,\tilde{\zeta}_i\,\tilde{\omega}_i \end{bmatrix} \quad ; \quad \tilde{\tilde{\mathbf{D}}}_{\mathrm{v}i}(t) = \mathbf{D}_{\mathrm{v}i}(t) - \mathbf{v}\,\mathbf{v}^{\mathrm{T}}\,M_{\mathrm{v}i}(t)\,\tilde{\mathbf{D}}_i$$

while the remaining quantities in Eqs. (A.33) take the same expressions as in Eqs. (23).

Appendix II. Review of the Dimensional Analysis

The basis of the Dimensional Analysis is that the form of any 'physically meaningful' equation has to be such that the relationship between the actual physical quantities is independent of the magnitude of the base units. This is because the value of a physical quantity, Q_0, that is an 'output variable' in a physical process, follows uniquely once all the 'input variables' that define the process, Q_1, Q_2, $\cdots$ and Q_r, are specified.

In this framework, the so-called 'Buckingham Π-Theorem' plays a fundamental role [28, 29]. The latter can be expressed as:

Any physically meaningful equation $Q_0 = \Phi(Q_1,\cdots,Q_r)$, involving a set of r input variables, is equivalent to a dimensionless equation of the form $\Pi_0 = \Psi(\Pi_1,\cdots,\Pi_{r-s})$, involving a set $r - s$ independent dimensionless combinations of the original r input variables, where s is the number of these input variables that are dimensionally independent.

The important fact to notice is that the new relation Ψ involves s fewer variables than the original relation Φ: this simplify the theoretical and experimental studies, and allows highlighting what really matter in a physical process.

According to Sonin [29], in the practical application of the Buckingham Π-Theorem, four steps have to be done:

1. The complete set of the input variable, $\{Q_1,\cdots,Q_r\}$, that determines the value of the output variable Q_0 is identified.

2. The dimensions of the input variables $\{Q_1,\cdots,Q_r\}$ are listed; a complete subset of dimensionally independent variables $\{Q_1,\cdots,Q_s\}$ ($s \leq r$) is selected among the input variables; the dimensions of each of the remaining input variables, $\{Q_{s+1},\cdots,Q_r\}$, and of the output variable, Q_0, are expressed as product of powers of the dimensions of $\{Q_1,\cdots,Q_s\}$, i.e.:

$$\left[Q_i \right] = \left[Q_1^{N_{i1}} \cdots Q_s^{N_{is}} \right] \quad , \quad i = 0, s+1, \cdots, r$$

where the exponents $N_{i1} \dots N_{is}$ are dimensionless real number.

3. The independent dimensionless combinations are defined:

$$\Pi_i = \frac{Q_{s+i}}{Q_1^{N_{(s+i)1}} \cdots Q_s^{N_{(s+i)s}}} \quad , \quad i = 1, \cdots, r-s \tag{A.34}$$

along with the dimensionless form of the output variable:

$$\Pi_0 = \frac{Q_0}{Q_1^{N_{(s+i)1}} \cdots Q_r^{N_{(s+i)s}}}$$

4. The dimensionless relationship $\Pi_0 = \Psi(\Pi_1, \cdots, \Pi_{r-s})$ can be established.

References

[1]   Frýba L., 1996. *Dynamics of railway bridge.* Telford, London, UK.

[2]   Yang Y.B., Yau J.D., Wu Y.S., 2004. *Vehicle-Bridge Interaction Dynamics.* World Scientific, River Edge, NJ.

[3]   Frýba L., 1999. *Vibration of solids and structures under moving loads*, 2nd Ed. Telford, London, UK.

[4]   Timoshenko S., Young D.H., Weaver W., 1974. *Vibration Problems in Engineering*, 4th Ed. John Wiley, New York, NY.

[5]   Warburton G.B., 1976. *The Dynamic Behaviour of Structures.* Pergamon Press, Oxford, UK.

[6]   Thambiratnam D., Zhuge Y, 1996. Dynamic analysis of beams on an elastic foundation subjected to moving loads. *Journal of Sound and Vibration* **198**, 149-69.

[7]   Felszeghy S.F., 1996. Timoshenko beam on an elastic foundation and subject to a moving step load, Part 2: Transient response. *ASME Journal of Vibration and Acoustics* **118**, 285-91.

[8]   Felszeghy S.F., 1996. Timoshenko beam on an elastic foundation and subject to a moving step load, Part 1: Steady-state response. *ASME Journal of Vibration and Acoustics* **118**, 277-84.

[9]   Chen Y.-H., Huang Y.-H., 2003. Dynamic characteristics of infinite and finite railways to moving loads. *Journal of Engineering Mechanics – ASCE* **129**, 987-995.

[10]   Cheng Y.S., Au F.T.K., Cheung Y.K., 2001. Vibration of railway bridges under a moving train by using bridge-track-vehicle element. *Engineering Structures* **23**, 1597-1606.

[11]   Biondi B., Muscolino G., Sofi A. A substructure approach for the dynamic analysis of train-track-bridge system. *Computer and Structures* **83**, 2271-81.

[12]   Bruni S., Collina A., 2000. Modelling the viscoelastic behaviour of elastomeric components: an application to the simulation of train-track interaction. *Vehicle System Dynamics* **34**, 283-301.

[13]   Nashif A.D., Jones D.I.G., Henderson J.P., 1985. *Vibration Damping.* Wiley, New York, NY.

[14]   Sun C.T., Lu Y.P., 1995. *Vibration Damping of Structural Elements.* Prentice Hall, Englewood Cliffs, NJ.

[15]   Palmeri A., Ricciardelli F., Muscolino G., De Luca A., 2004. Effects of viscoelastic memory on the buffeting response of tall buildings. *Wind & Structures* **7**, 89-106.

[16]   Inaudi J.A., Kelly J.M., 1995. Modal equations of linear structures with viscoelastic dampers. *Earthquake Engineering and Structural Dynamics* **24**, 145-51.

[17]   Caughey T.K., O'Kelly N.E.J., 1965 Classical normal modes in damped linear dynamic systems. *Journal of Applied Mechanics – ASME* **32**, 583-8.

[18]   Palmeri A., Ricciardelli F., De Luca A., Muscolino G., 2003. State space formulation for linear viscoelastic dynamic systems with memory. *Journal of Engineering Mechanics – ASCE* **129**, 715-24.

[19]   Szidarovszky F., Bahill A.T., 1998. *Linear Systems Theory*, 2nd Ed. CRC Press, Boca Raton, FL.

[20]   Borino, G., Muscolino G., 1986. Mode-superposition methods in dynamic analysis of classically and non-classically damped linear systems. *Earthquake Engineering and Structural Dynamics* **14**, 705-17.

[21]   Muscolino G., 1996. Dinamically modified linear structures: deterministic and stochastic response. *Journal of Engineering Mechanics – ASCE* **122**, 1044-51.

[22]   Wolfram Research, 1999. *Mathematica* 4.0, Champaign, IL, <http://www.wolfram .com>.

[23]   Johnson C.D., Kienholz. D.A., 1982. Finite element prediction of damping in structures with constrained viscoelastic layers. *AIAA Journal* **20**, 1284-90.

[24]   Palmeri A., Ricciardelli F. The fatigue limit state in building with viscoelastic dampers. *Journal of Wind Engineering and Industrial Aerodynamics* **94**, 377-95.

[25]   Palmeri A. Correlation coefficients for viscoelastically damped structures. *Engineering Structures* **28**, 1197-208.

[26]   Makris N., and Zhang J., 2000. Time domain viscoelastic analysis of earth structures. *Earthquake Engineering and Structural Dynamics* **29**, 745-68.

[27]   Muscolino G., Palmeri A., Ricciardelli F. 2005. Time-domain response of linear hysteretic system to deterministic and random excitation. *Earthquake Engineering and Structural Dynamics* **34**, 1129-48.

[28]   Barenblatt G.I., 1996. *Scaling, Self-Similarity, and Intermediate Asymptotics*. Cambridge University Press, New York, NY.

[29]   Sonin A.A., 2001. *The Physical Basis of Dimensional Analysis*, 2nd Ed. Massachusetts Institute of Technology, Cambridge, MA, <http://web.mit.edu/2.25 /www/pdf/ DA_unified.pdf>.

List of figures:

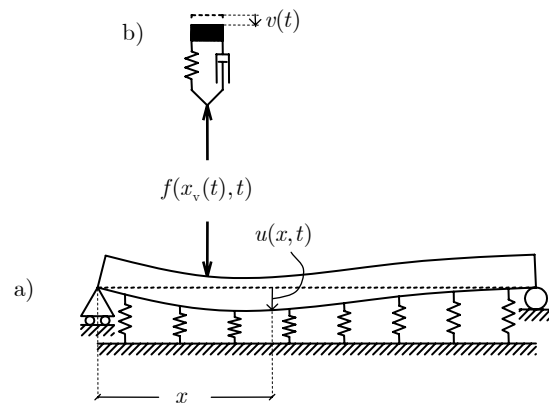Figure 1. Schematic of a beam on viscoelastic foundation carrying a SDoF moving oscillator.

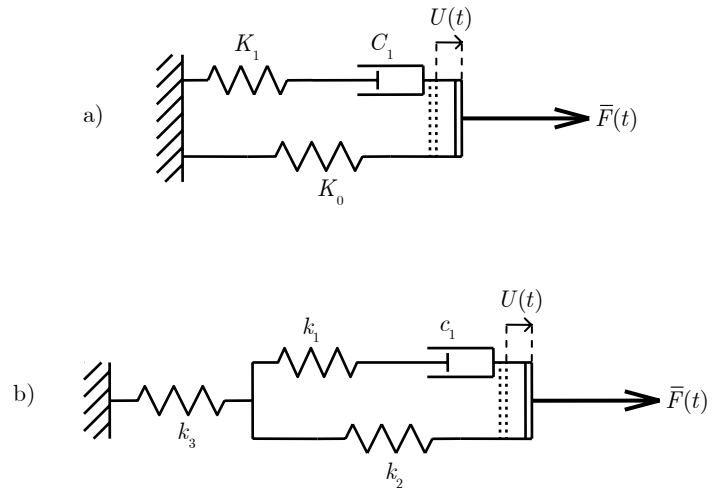Figure 2. Interaction between beam-foundation sub-system (a) and moving oscillator (b).

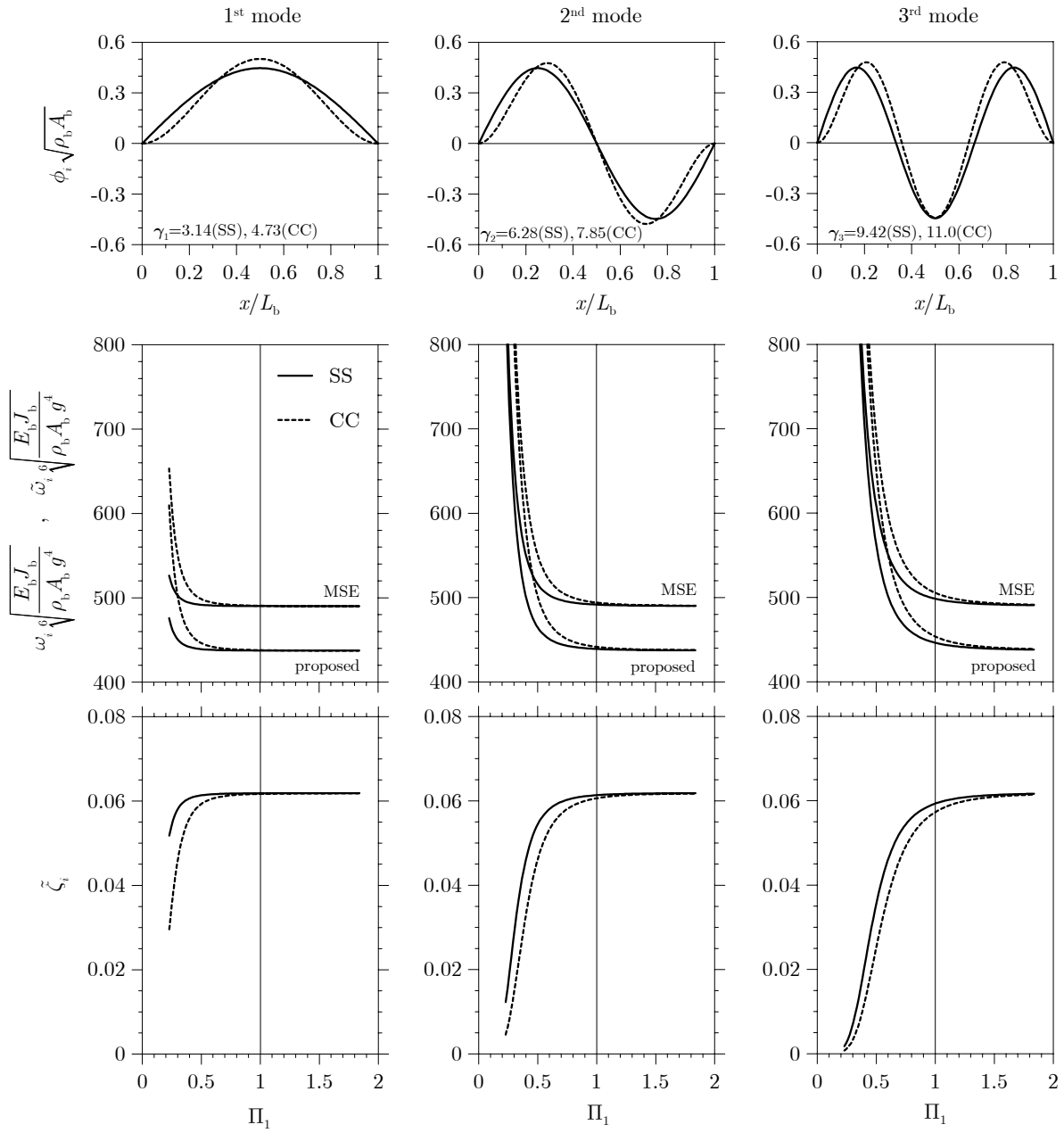Figure 3. Standard Linear Solid (SLS) model (a) and Zener model (b).

Figure 4. Modal shapes of the beam-foundation sub-system (top rows). Effects of the span length of the beam ($\Pi_1 \propto L_b$) on frequencies (centre rows) and effective damping ratio (bottom rows) of the first modes. ----- Simply Supported (SS) beam. - - - Clamped-Clamped beam.
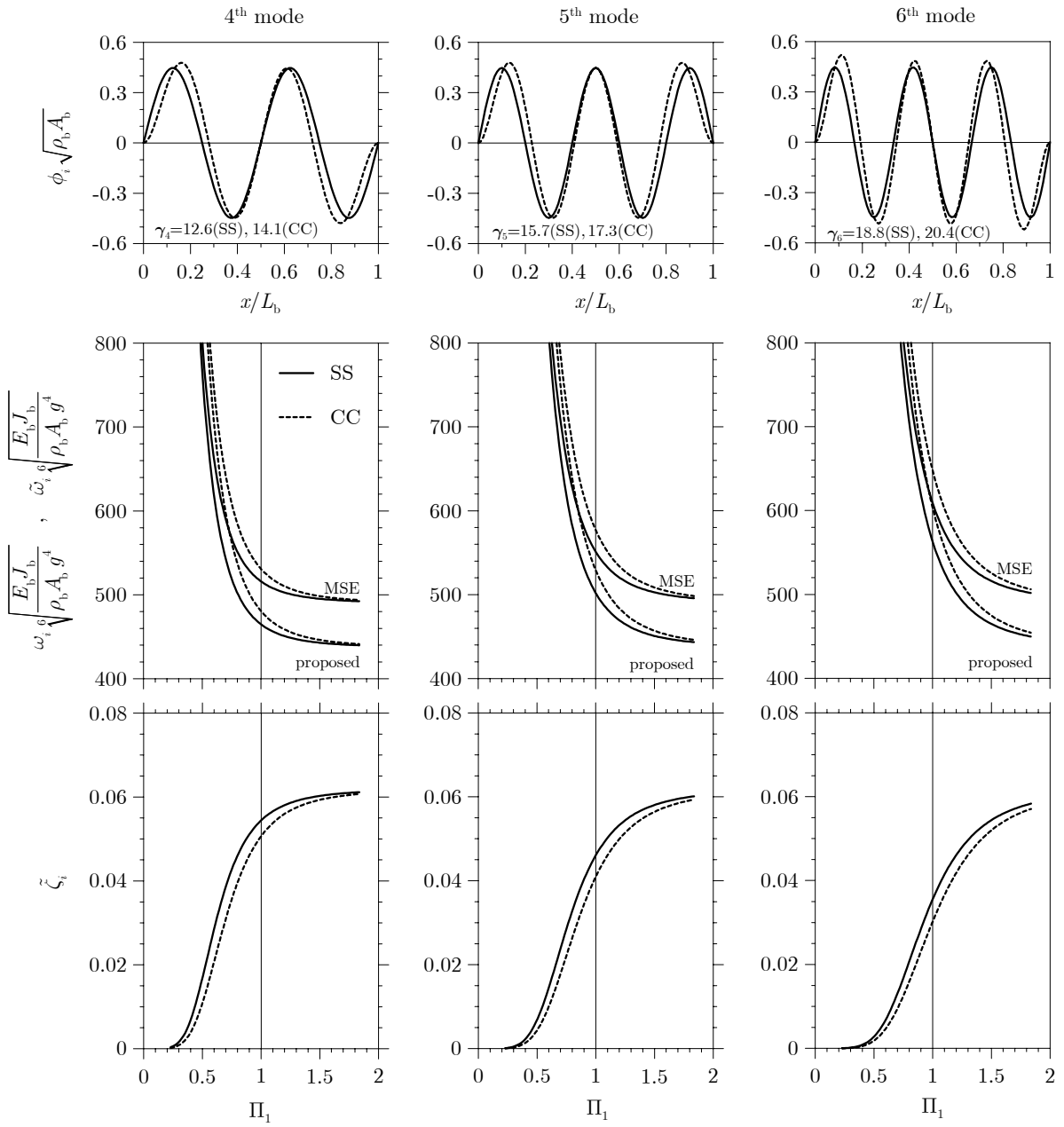
Figure 4. Continues.
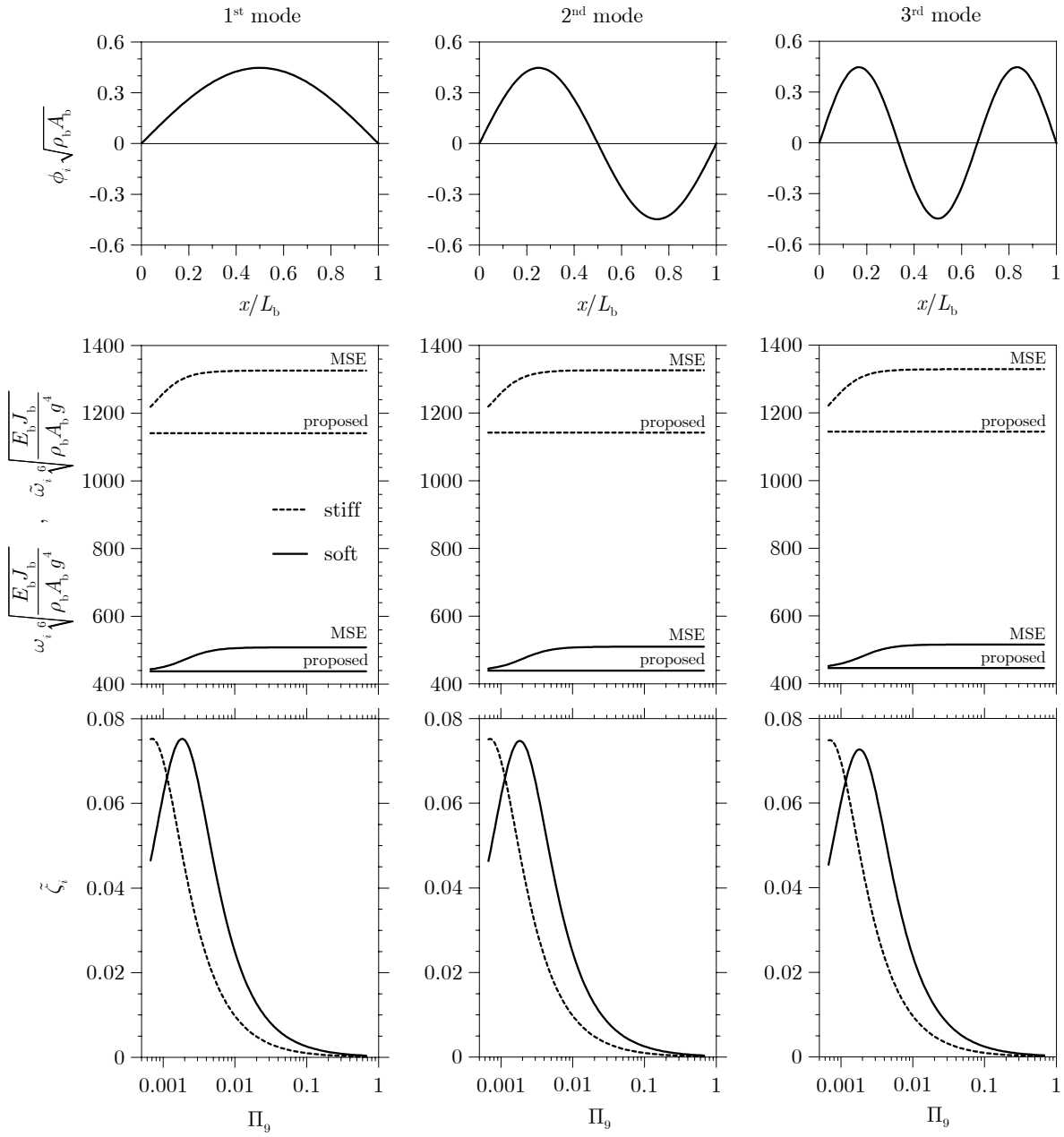
Figure 5. Modal shapes of the beam-foundation sub-system (top rows). Effects of the relaxation time of the viscoelastic foundation ($\Pi_9 \propto \tau_1$) on frequencies (centre rows) and effective damping ratio (bottom rows) of the first modes. ----- Soft foundation. - - - Stiff foundation.
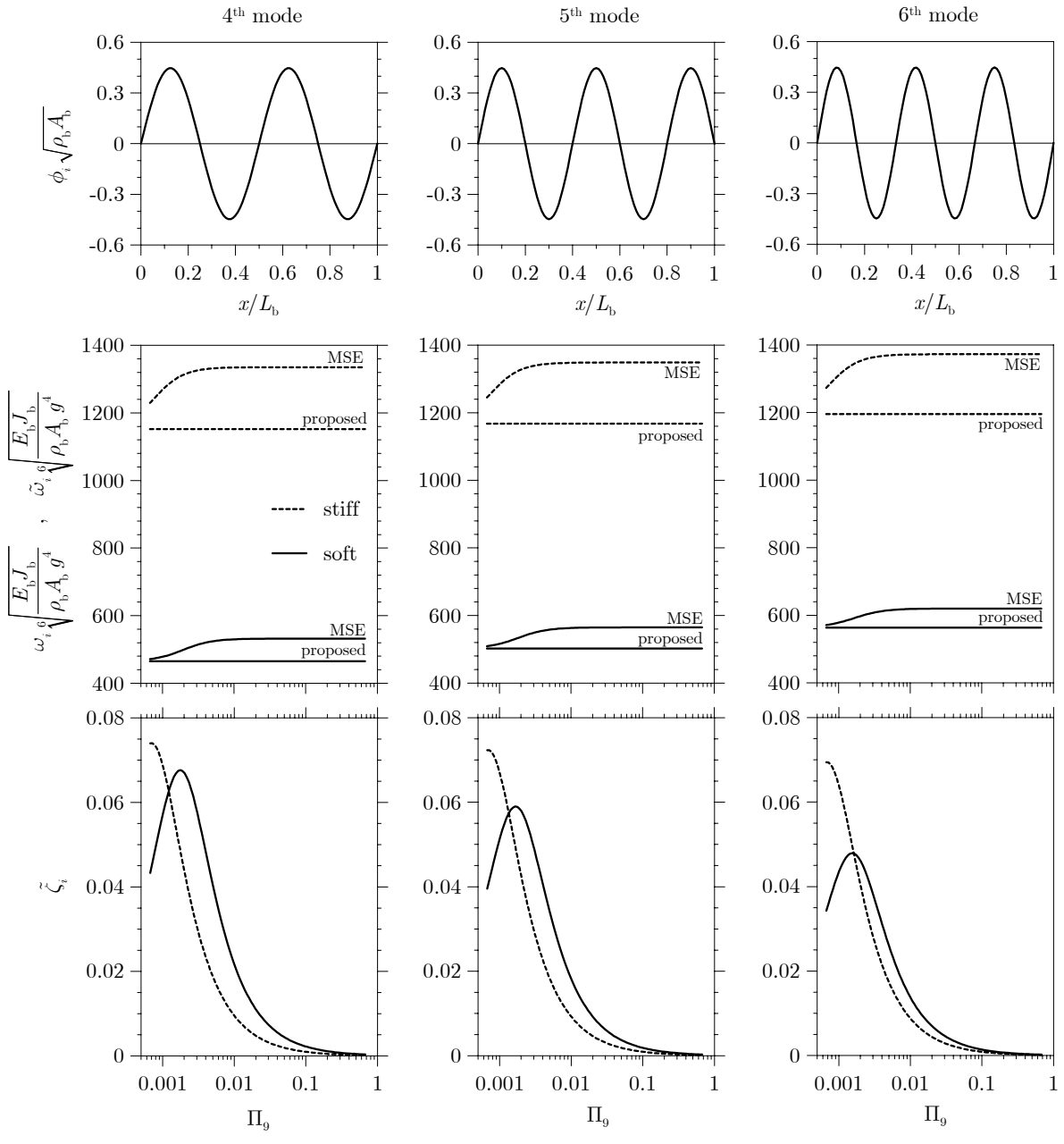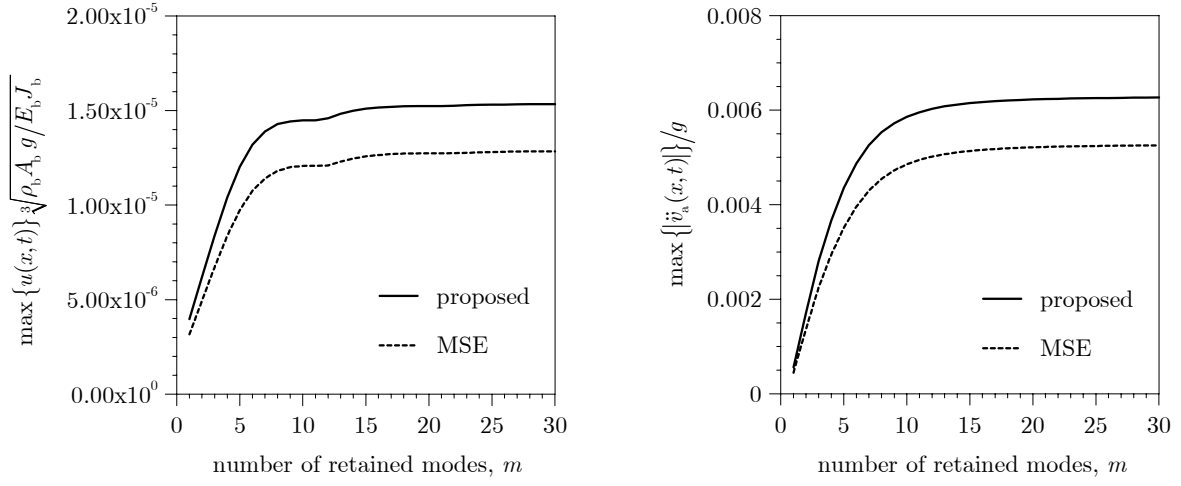
Figure 5. Continues.

Figure 6. Convergence of the dimensionless peak responses of beam (left) and oscillator (right) when the number of modes retained in the analysis increases.
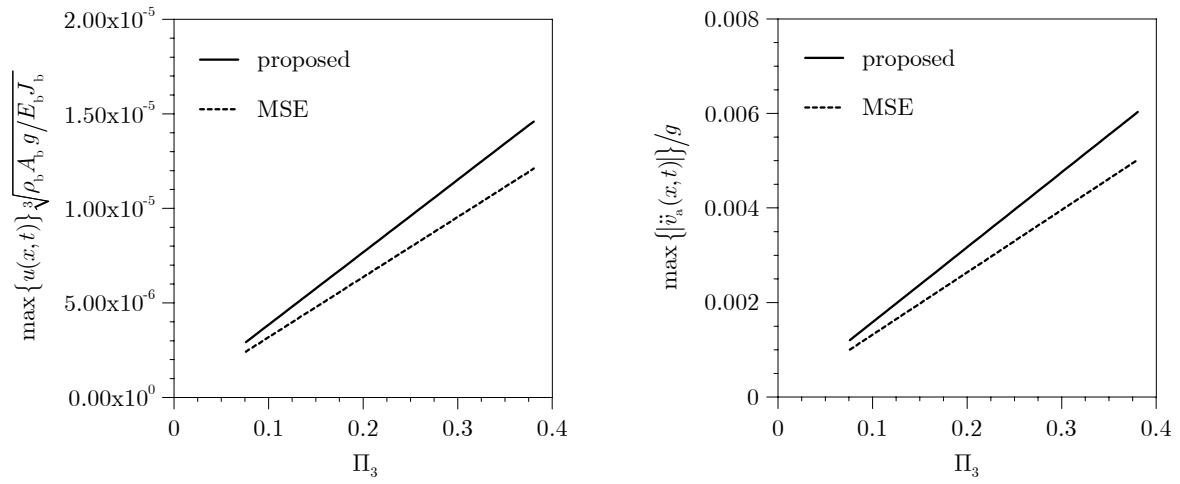
Figure 7. Effects of the mass of the oscillator ($\Pi_3 \propto m_v$) on the dimensionless peak responses of beam (left) and oscillator (right).
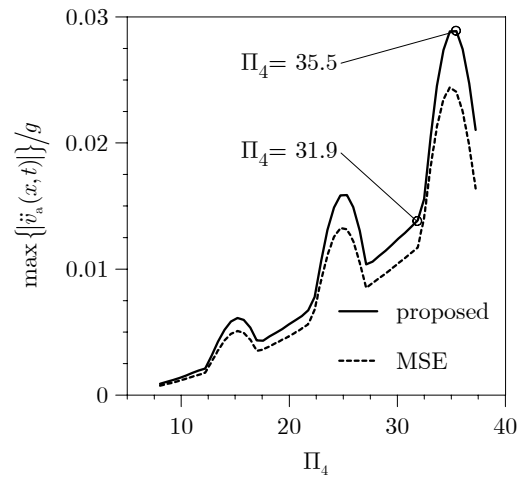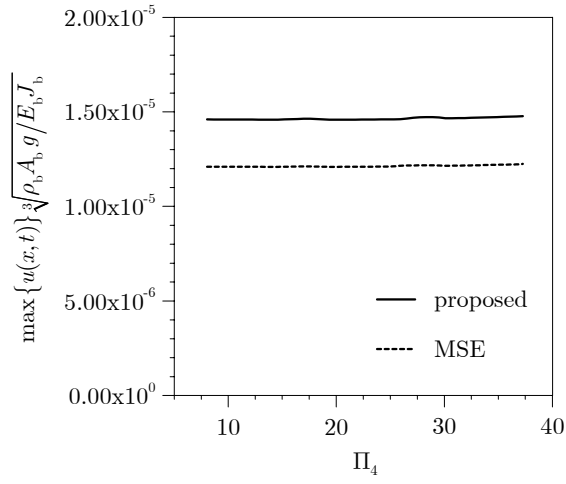
2.00×10^{-5}

1.50×10^{-5}

1.00×10^{-5}

5.00×10^{-6}

0.00×10^{0}

$\max\{u(x,t)\}\sqrt[3]{\rho_b A_b\, g/E_b J_b}$

proposed

MSE

10   20   30   40

Π_4

0.03

0.02

0.01

0

$\max\{|\ddot{v}_a(x,t)|\}/g$

$\Pi_4 = 35.5$

$\Pi_4 = 31.9$

proposed

MSE

10   20   30   40

Π_4

Figure 8. Effects of the circular frequency of the oscillator ($\Pi_4 \propto \omega_v$)
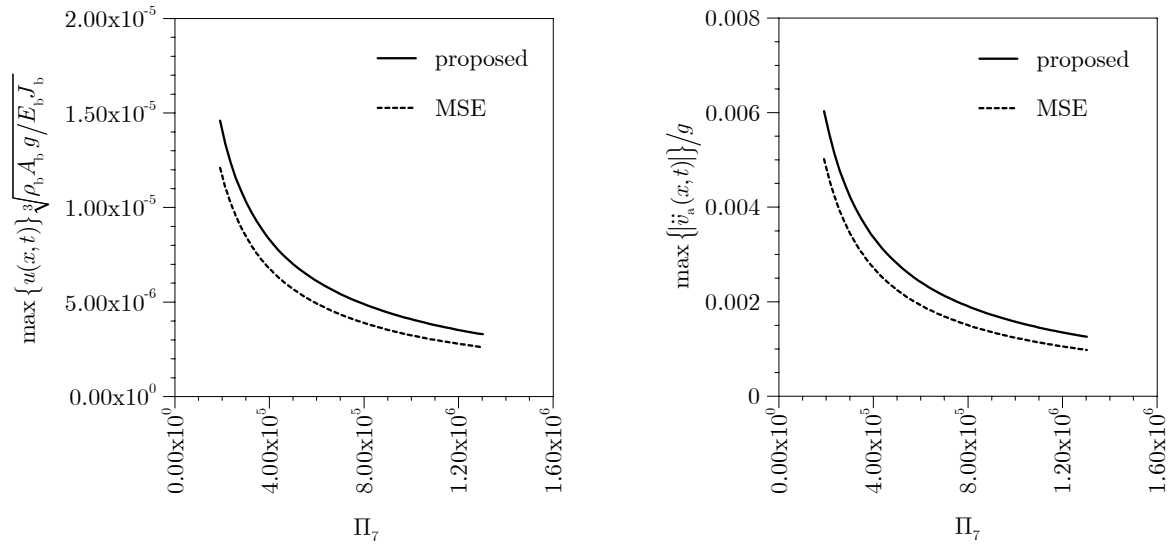on the dimensionless peak responses of beam (left) and oscillator (right).

Figure 9. Effects of the equilibrium modulus of the foundation ($\Pi_7 \propto K_0$) on the dimensionless peak responses of beam (left) and oscillator (right).
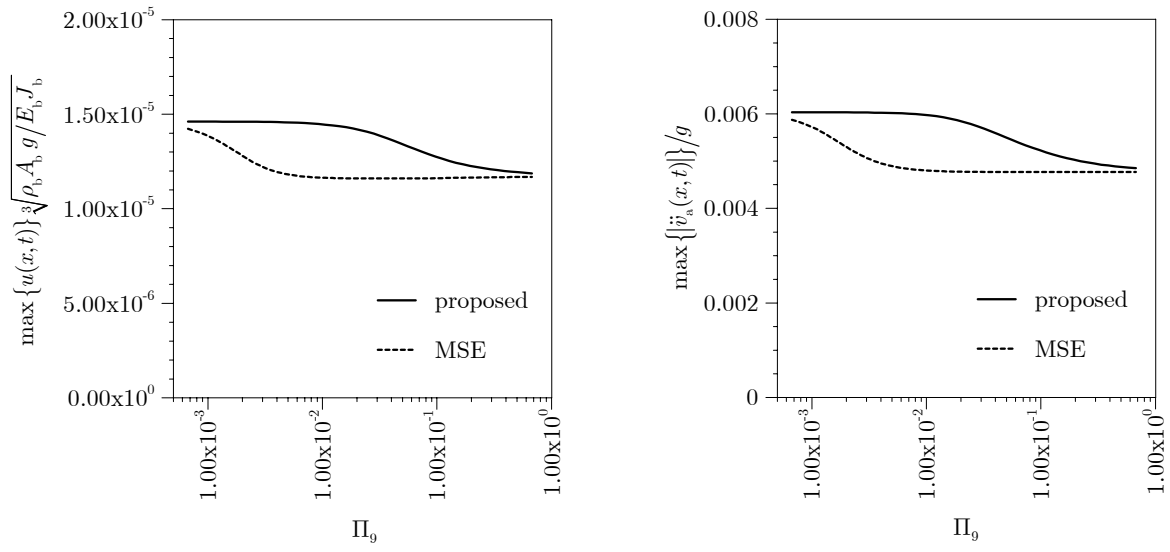
Figure 10. Effects of the relaxation time of the foundation ($\Pi_9 \propto \tau_1$) on the dimensionless peak responses of beam (left) and oscillator (right).